Crude oil inventory estimation using remote sensing

Stud.tech. Valdemar Edvard Sandal Rolfsen

Desember 2017

Specialization Report

Department of Civil and Transport Engineering, Division of Geomatics
Faculty of Engineering Science and Technology
Norwegian University of Science and Technology

Supervisor 1: Terje Midtbø

Supervisor 2: Erik Wold

Abstract

Cushing, Oklahoma, a major crude oil trading hub, is often referred to as the famous price settlement point for West Texas Intermediate of the New York Mercantile Exchange. It lies a significant economic potential in knowing the inventory numbers of this area before they are released.

This paper investigates different approaches to estimate the total inventory using remote sensing techniques, including standard approaches for semantic segmentation, machine learning, height estimation using SAR and InSAR analysis and trigonometrical height estimation using building shadows cast by the sun.

These methods are then compared, evaluated and combined to find the approach that is most likely suitable for accurately retrieving the inventory numbers.

Preface

This report is a result of the specialization project TBA4560, at the Division of Geomatics, NTNU. The project was carried out the autumn of 2017 in cooperation with Rystad Enery, an international oil and gas knowledge house. The main supervisor has been Terje Midtbø, and Erik Wold the CTO of Rystad Energy has been the assisting supervisor.

Through the project the author has gotten a good understanding of the principles behind semantic segmentation and height estimation, and which methods that can be used to extract information from remote sensing data. Especially the field of machine learning has been very interesting to explore, because of the enormous potential that lies within its applications.

In general, the author feel that the project has provided a good insight as to how to write good and concise reports.

Trondheim, 2017-12-20

Valdemar Edvard Sandal Rolfsen

Contents

Chapter 1

Introduction

Semantic segmentation and feature extraction in remote sensing has been a field of research for many decades. The ability to extract geospatial information directly from satellite imagery has been crucial for areas such as environmental and demographic research. Furthermore, a vast development within the field of machine learning and artificial intelligence the last years has enabled many researchers to find useful applications of such algorithms within their scientific fields.

With new satellite technology providing frequently updated imagery, with resolutions less than 0.5 meters, the amount of data that can be extracted is almost incomprehensible. This paper focuses on how automatic height estimation of ground objects can be achieved through remote sensing, semantic image segmentation, and different height estimation techniques.

The primary goal of this study is to investigate different methods for automatic detection and height retrieval of the roofs of oil tanks in Cushing, Oklahoma. By knowing the height difference between the tanks floating roofs and their actual height, it is possible to calculate their inventory.

1.1 Background

Satellites have been collecting earth observation data for decades. Since the satellite Explorer 6 took the first picture of the earth in 1959, millions of satellite images have been captured, processed and stored Esa (2009). This information has been difficult to access, and even harder to analyze when accessible. However, during the last decade, the development of machine learning based methods for Earth Science applications has experienced a considerable leap forward Lary (2010).

In 2014 the first satellite in the new family of earth observation satellites, called the Sentinels, was launched from Kourou, French Guiana. Since then seven different constellations, each consisting of two satellites, have been launched, and are now orbiting and monitoring the earth's surface. The goal of these satellites is to produce a continuous stream of timely data for Europe's Copernicus program, which will be used for environmental monitoring. The different constellations have different missions when it comes to providing datasets for the Copernicus Service. While some are focused on specific data, such as monitoring the earth's atmosphere, other constellations offer more general data, such as multi-spectral, high-resolution imagery of the earth's surface. In order to maximize the usage of these temporal datasets, they have all been provided free of charge to the public. Other satellite constellations such as SkySat (Planet, 2017) and WorldView (DigitalGlobe, 2017) provide even more accurate satellite imagery, with submeter resolutions. With these satellites providing frequently updated imagery over most parts of the earth's surface, the amount of earth observation data that can be observed is enormous.

The development of these satellite constellations means that data that earlier required manual measurements to be analyzed, now can be gathered, processes and analyzed automatically at a high phase. One field where this can provide valuable information is within the oil industry.

Cushing Oklahoma is the major trading hub and famous price settlement point for West Texas Intermediate of the New York Mercantile Exchange. With inventory numbers not being continuously updated by Energy Information Administration (EIA), there exists a potential in retrieving these numbers automatically through remote sensing.

Figure 1.1: Oil tanks with different amounts of oil inventory

1.2 Problem

The paper aims to answer if it is possible, with today's methods and satellite technology to automatically provide frequently updated estimations of the total inventory of all the crude oil tanks in Cushing, Oklahoma.

1.3 Approach

This paper will focus on investigating the theory and previous work related to semantic segmentation of satellite images and techniques for height detection using data collected through remote sensing. By combining these two fields of research, it is theorized that it can be possible to automatically locate and estimate the inventory of oil tanks in Cushing, Oklahoma.

Semantic segmentation

Regarding semantic segmentation, the paper discusses different approaches ranging from standard methods, such as the Hough transform to newer, more advanced techniques such as image segmentation using convolutional neural networks. The goal is to present the strengths and weaknesses of the different methods, to determine which one is most suitable for the task at hand.

Height estimation

There are also a large variety of different methods for height estimation using data from satellite imagery. While the methods investigated related to semantic segmentation only focus on multispectral images, both techniques using radar images and multispectral imaged are considered for height estimation. The methods that are examined are SAR, InSAR and shadow measurements.

1.4 Limitations

This study is conducted as a literature review and does not present any implementation of the methods that are investigated.

1.5 Outline

The remaining part of this paper consists of the following chapters:

- Chapter 2. Theoretical background: This chapter gives a theoretical background of the different methods that are investigated later in the paper. It provides the necessary knowledge required to understand the various methods presented in related work.
- Chapter 3. Related Work: In this chapter, the previous work relevant to this paper is presented. It includes standard methods for image segmentation, an overview of the advances in convolutional neural networks and how they can be used for image segmentation. Furthermore, different works related to height estimation of buildings are presented.
- Chapter 4. Evaluating the methods: The focus of this chapter is to evaluate and compare the different methods that have been investigated in the previous chapters.
- Chapter 5. Conclusions, discussion, and ideas for further work: A conclusion is presented based on the previous chapters and some future work is presented.
- Bibliography

Chapter 2

Theoretical background

In this chapter, we are going to investigate some of the fundamental concepts related to pattern recognition, shape detection in imagery and height estimation from remote sensing.

2.1 Image segmentation

Identifying geometric shapes in computer vision has been a classical problem for decades. There are many theories related to what is the best way of detecting a particular shape in an image, with shapes defines as two-dimensional features of an object that are invariant to scene factors, or whose variation can be modeled easily (Moon et al., 2002).

2.1.1 The Hough transform

In image analysis, the Hough Transform is a technique used for feature extraction. This method uses a voting procedure from which object candidates are obtained as local maxima in a space constructed by the algorithm (called an accumulator space). Since the algorithm requires that the desired features are specified in some parametric form, the classical Hough transform is mostly used for the detection of regular curves (lines, circles ellipses, etc.).

The main idea of the algorithm is that each edge pixel contributes to a globally consistent solution, such as a curve. To detect a points contribution to this solution, the algorithm performs a point-to-curve transformation from the cartesian image coordinate space, to a polar Hough parameter space. In the cartesian coordinate space, a line segment can be represented by Equation 2.1.

$$xcos(\theta) + ysin(\theta) = r \tag{2.1}$$

In Figure 2.2 each point (x,y) on the line corresponds to a set of constant r and θ values.

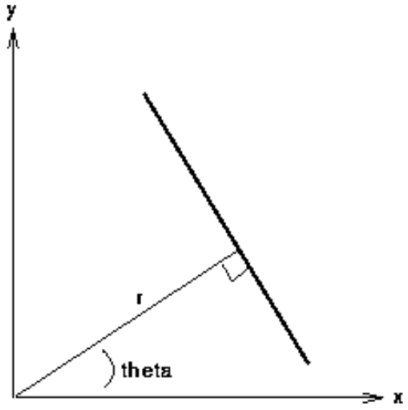

Figure 2.1: Parametric line represented by Equation 2.1 (Fisher et al., 2003)

Therefore when viewed in the Hough parameter space, points that are collinear in the cartesian space will yield curves which intersect at common r and θ values. Here bright areas (high degree of intersection) indicates collinearity between points in an image.

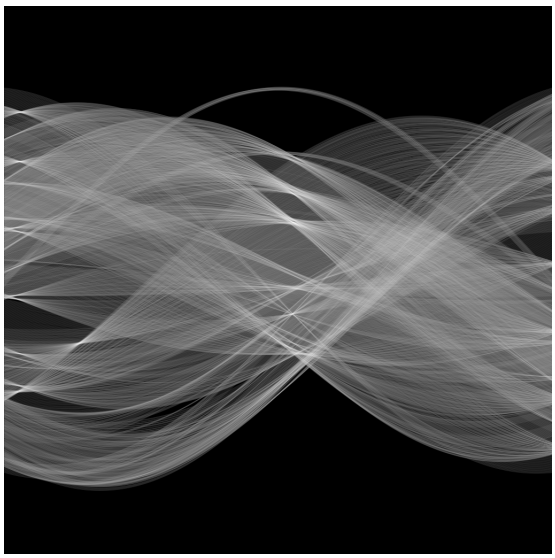

Figure 2.2: Parametric line represented by Equation 2.1 (Fisher et al., 2003)

For detecting circles the computational complexity of the algorithm increases, because the parametric equation representing a circle requires a three dimensional Hough parameter space (see Equation 2.2).

$$(x-a)^2 + (y-b)^2 = r^2 \tag{2.2}$$

2.1.2 Image segmentation using superpixels

Most images are based on a raster format, meaning that pixels in the image are structured as an array or grid, where each pixel is associated with a position (row and column), and a numeric value. Raster images can represent a range of different shapes, where a point can be represented by a single pixel and a circle by a contiguous collection of pixels (Worboys, 2003). Even though raster images are easy to work with in most computer systems, since they are represented the way that they are, they do not contain any information about the topology of the objects in the image. For example, there is no way of knowing if a pixel is contained within a particular object or not. An approach to detecting objects is therefore to detect edge pixels.

In recent years shape detection algorithms have come to increasingly rely on superpixel algorithms, which groups pixels into perceptually meaningful atomic regions (Achanta et al., 2012). Such regions replace the regular, rigid structure of the raster grid, as shown in Figure 2.3.

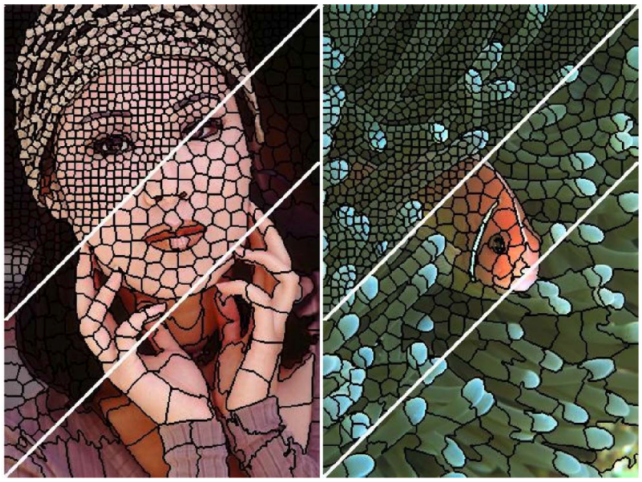

Figure 2.3: Visualization of image segmentation using SLIC (Achanta et al., 2012)

When constructing superpixels, there are some properties of the algorithm that is desirable, regardless of the problem that is being solved. These are, according to (Achanta et al., 2012), the following three points:

- Superpixels should adhere well to image boundaries
- When used to reduce computional complexity as a preprocessing step, superpixels should be fast to compute, memory efficient, and simple to use.

- When used for segmentation purposes, superpixels should both increase the speed and improve the quality of the results.

2.2 Artificial Neural Networks

In recent years, the development of machine learning, a branch of artificially intelligent systems, has become increasingly important regarding pattern and object recognition in remote sensing and image analysis in general. One of the most commonly used approaches for data mining in remote sensing has been artificial neural networks Lary et al. (2016).

The fundamental principle behind artificial neural networks (ANNs) is that it is built up by a network of many simple units that are working in parallel with no centralized control unit. The networks primary means of storage are the weights between the individual units, and the network learns by updating these weights every time it is provided with a training example.

In order to understand the behavior of ANNs it is important to understand their structures. The most common structure for an ANN is what is called a Feed-forward neural network structure.

2.2.1 Feed-forward neural networks

A feed-forward neural network is build up by a given number of connected layers. A layer is a collection of simple units, called artificial neurons. All networks must consist of one input and output layer, but can also contain an optional number of hidden layers. A network that only consists of one input and output layer is called a perceptron, and it has been shown that these types of networks are only able to model linear functions (Minsky and Papert, 1969).

Input Layer The input layer is the layer that feeds the information into the network. Here the number of neurons is typically equal to the number of features in the data.

Hidden layer The hidden layers in an ANN are what enables the network to learn and model nonlinear functions. It is the weights on the connections between the different layers that enables the network to encode the information extracted from the training data.

Output layer An output layer has to be present in order to extract the answer or prediction from the model. Depending on the setup of the neural network, the output value can either be a real value or a set of probabilities. The output type is dependent on the activation that is

chosen for the layer. What an activation function is, and how it effects the output of a layer will be discussed later in this section.

A feed-forward network can either be fully or partly connected. In a fully connected network, all the neurons in each layer have a connection to all neurons in the previous layer, and all neurons in the next layer, while in a partly connected layer only some of the neurons are connected.

2.2.2 Training a neural network

The primary purpose of a well trained ANN is to be able, by using its weighted connections, to amplify the signal and dampen the noise of the data it has been trained on. It does so by altering the different weights and biases in a way that allocates significance to some features and removing it from other. This way the model can learn which features are tied to which outcomes.

Neural networks learn these relationships by making a guess based on the input, weights, and biases, and then get feedback on how accurate the guess was. It is the loss function related to the model, such as stochastic gradient descent (SDG), which gives this feedback by rewarding good guesses and penalizing bad ones.

The most common learning algorithm associated with neural networks is the *backpropagation learning algorithm.*

Backpropagation learning

The backpropagation algorithm learns by first trying to compute a training examples output value, by taking a forward pass through the network. If the output matches the label associated with the example nothing happens, but if it does not the weights has to be updated.

In order to update the weights in the network, Equation 2.3 is used.

$$W_{j,i} \Leftarrow W_{j,i} + \alpha * a_j * Err_i * g'(input\_sum_i) \tag{2.3}$$

Equation 2.3 is called the weight update rule for the connection between neuron j and i as seen in Figure 2.4. Furthermore, α is the learning rate (discussed in subsection 2.2.5), a_j is the incoming activation function, Err_i is the error in i and $g'(input\_sum_i)$ is the derivative of the activation function over the input sum as seen in Equation 2.4.

$$a_j = g(input\_sum_j) \tag{2.4}$$

where the input sum is given by:

$$input\_sum_i = W_i * A_i + b \tag{2.5}$$

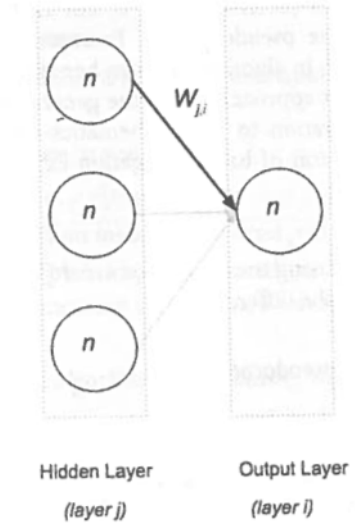

Figure 2.4: The two last layers of an multilayer feed-forward neural network Patterson and Gibson (2017)

The backpropagation algorithm traverses the network backward, updating the weight of connection between each layer, as described in Equation 2.3 until it reaches the input layer. This way the weights and biases that have been assigned the blame for the error are reduced, while the ones that are supporting the correct answer are strengthened.

2.2.3 Activation functions

Activation functions are scalar-to-scalar functions which are used to propagate the output of one layer to the next, and it is what enables the network to model nonlinear functions. This section will discuss some of the most common activation functions used in ANNs.

Linear The linear activation function, $f(x) = Wx$ is the most straightforward activation function and is often associated with the input layer of the network. It says that the dependent variable x is proportional to the independent variable Wx.

Sigmoid The sigmoid activation function belongs to the class of logistic activation functions. It reduces extreme values or outliers in the example data, without removing them. One could see the sigmoid function as a machine that coverts independent variables of near infinite range into probabilities between 0 and 1.

Tanh (and Hard Tanh) Another class of activation functions is the hyperbolic trigonometric functions. The tanh function represents the ratio between the hyperbolic sine sine to the hyperbolic cosine, which means that unlike the sigmoid function, it has a normalized range between -1 and 1. The hard tanh activation function simply adds hard caps to the range, setting all values larger than 1 and smaller than -1 to respectively 1 and -1. The advantage of these functions is that they can deal more efficiently with negative numbers.

Softmax The softmax function also referred to as the normalized, exponential function, is a generalization of the logistic function. Its function is that it returns the probability distribution over mutually exclusive output classes. For example, if the softmax activation function was applied to the vector [1, 2, 3, 4, 1, 2, 3], the result would be [0.024, 0.064, 0.175, 0.475, 0.024, 0.064, 0.175,]. As seen from this example, the function is most often used to weight the largest value and dampen values that are considerably smaller.

ReLU The rectified linear unit function is currently considered the state of the art activation function. It can be described as $f(x) = max(0, x)$, meaning that it, above a certain threshold the output has a linear relationship with the dependent variable, it is else zero.

2.2.4 Loss functions

When working with artificial neural networks, we often talk about the ideal state of the network, meaning the state that classifies all the examples correctly. The loss function is a way of quantifying how close a network is to this ideal state. This is done by aggregating the errors produced by the network's prediction over the entire dataset and average this value to get a single number that represents how close the network is to its ideal state. In other words, by minimizing the loss function, the network gets as close as possible to its ideal state, resulting in an optimization problem where the solution can be approximated well with iterative optimization algorithms.

There are different loss functions that are appropriate for regression and classification problems, however, for this project report, it is only relevant to discuss the ones related to classification problems.

Hinge loss For hard classification, for example with discrete classes [sell=0, buy=1], the hinge loss function is most commonly used. It is also used by a type of models called maximum-margin classification models such as support vector machines, which are discussed in **??**.

Logistic loss Often probabilities are of more significant interest than hard classifications, in such situations the logistic loss function is of more value. A vital remark when computing probabilities, is that all values have to be in the range 0 to 1 and that the probability of mutually exclusive outcomes should sum up to 1. Therefore, it is essential that the last layer uses the softmax activation function.

Optimizing the logistic loss function is the same as optimizing the "maximal likelihood", which means that the algorithm should maximize the probability that it predicts the correct class, and do so for every single sample in the dataset.

2.2.5 Hyperparamenters

In machine learning, hyperparameters deal with controlling the optimization functions during learning, making sure that they neither overfit or underfit the data, but at the same time learns as quickly as possible.

Learning rate The learning rate, as seen in Equation 2.3 is a coefficient that scales the size of each weight update step. In other words, the learning rate decides how much of the computed gradient that should be used for each step.

Regularization Regularization is essential to control what is called out-of-control parameters. This is done by controlling the trade-off between finding a good fit on the training data and limiting the weight of features with high-polynomials. This is because such features tend to overfit the training examples.

Momentum Momentum is often described as the learning rate of the learning rate. What it does is to prevent the learning algorithm from getting stuck in local minima.

Sparsity Lastly, the sparsity hyperparameter helps recognize which features of the input examples that are relevant. This is important because, in some datasets, the feature arrays for each sample will be very different regarding values.

2.2.6 Overfitting

An important concept within the field of machine learning is overfitting. We say that a hypothesis overfits its training data when there exists an alternative hypothesis with the same or higher training error that generalizes better.

In other words, overfitting refers to a hypothesis that models its training data too well. It learns the detail and the noise of the training data to the extent that it negatively impacts the performance of the hypothesis on new data. This means that the noise or random fluctuations in the training data is picked up and learned as concepts by the hypothesis. The problem is that these concepts do not apply to new data and negatively impact the hypothesis ability to generalize.

2.2.7 Convolutional neural networks

In recent years, convolutional neural networks (CNN's) have been recognized as very suitable for object recognition in images Patterson and Gibson (2017). One of the main reasons why the world, research society acknowledges the power of deep learning has been the efficiency of CNN's image recognition capabilities. The name comes from the networks use of convolutions, a mathematical operation on two functions to produce a third.

Biological Inspiration

Like all neural networks, CNN's are very inspired by the biological neurons in animal brains. The CNN's are mainly inspired by the visual cortex, which cells are very sensitive to small subregions of the input. One often says that these cells act as local filters over the input space, which also is the case for CNN's.

Difference from regular feed-forward multilayer neural networks

A well-known problem when it comes to analyzing image data using regular feed-forward multilayer neural networks is that they do not scale well with increasing image sizes. Imagine a color image with the size 400x400 pixels (which would be a regular sized picture) that are used as input for an ANN. Such an image, represented as a vector, would create $400 * 400 * 3 = 480000$ different weight connections for each neuron in the first hidden layer. For a fully connected network, this would be the case for all layers to come, which would create a tremendous amount of weight connections.

Convolutional neural networks solve this issue by representing the images in a three-dimensional structure, meaning that the input data is represented as a three-dimensional matrix with:

- Image width in pixels
- Image height in pixels
- RGB channels in depth

As will be discussed later, this structure is how CNN's have evolved from previous feed-forward networks, regarding computational efficiency.

Architecture

The purpose of the network is to transform the input examples through a series of connected layers, into a set of class scores. A general architecture is presented in Figure 2.6.

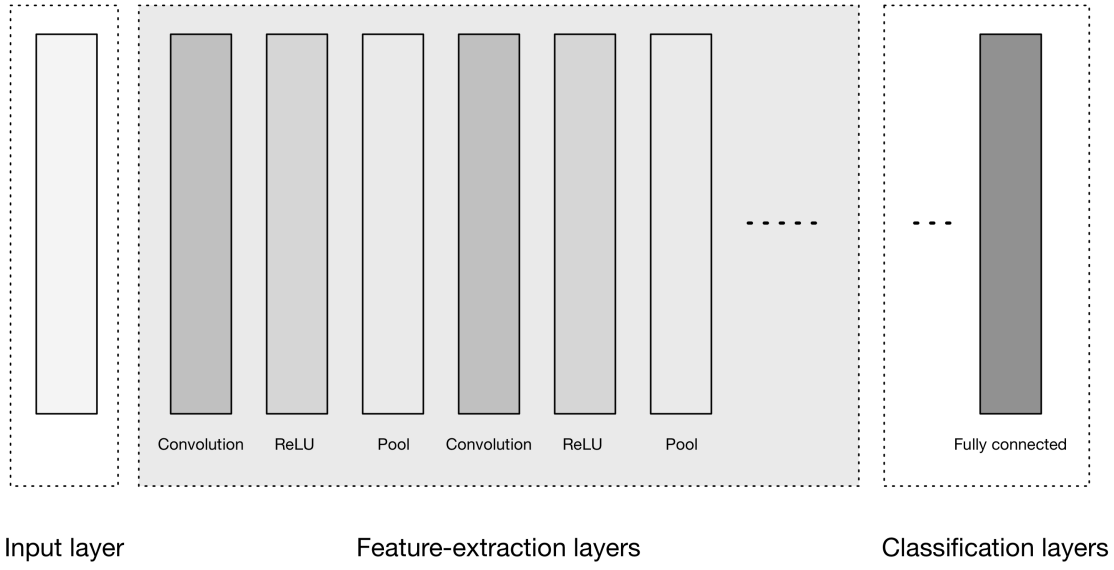

Figure 2.5: A general presentation of the architecture of CNNs Patterson and Gibson (2017)

As seen in Figure 2.6 the network can be divided into three sections; Input, Feature-extraction and Classification layer(s). The most interesting part of this structure is the feature-extraction layers, which is used to identify features in the images, and from these construct higher-order features. The strategy of constructing high-order features is one of the key aspects of deep learning.

Remark: It is important to note that in a CNN's layers, the neurons are arranged in a three-dimensional structure, to match the input data, as described earlier.

Convolutional layers

The convolution layers, seen in Figure 2.6, detect features in an image through what is called the convolution operation. As mentioned at the beginning of this chapter is a convolution operation a mathematical operation that transforms two functions (or sets of information) into one, through Fourier transformations. The way that this works is that the layer applies specific filters, called kernel filters, to segments of its input using a technique called sliding window.[1] The convolution operator is described in Equation 2.6, where I is the input data and K is the kernel filter of size $h * w$.

$$(I * K)_{xy} = \sum_{i=1}^{h} \sum_{j=1}^{w} K_{ij} \cdot I_{x+i-1,y+j-1} \tag{2.6}$$

Such filters can, for example, be an edge kernel, which only passes through information containing edges. In most cases applying a filter means reducing the size of the data, thus reducing the number of neurons in each, upcoming layer.

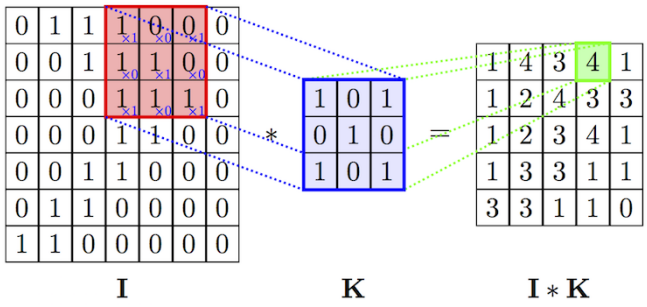

Figure 2.6: The convolution operation (applying a kernel filter) Cambridge (2017)

ReLU layers

As seen in Figure 2.6, ReLU activation functions are often used in separate layers. This layer does not change the dimension of the input volume but can change some of the pixel values.

[1] A technique that slides over a set of data, only analyzing a pre-defined patch size at a time Stanford (2017)

Pooling layers

The pooling layers is another important part of the convolutional neural networks. They help prevent overfitting, by reducing the size of the input data using what is called max pooling, as shown in Figure 2.7

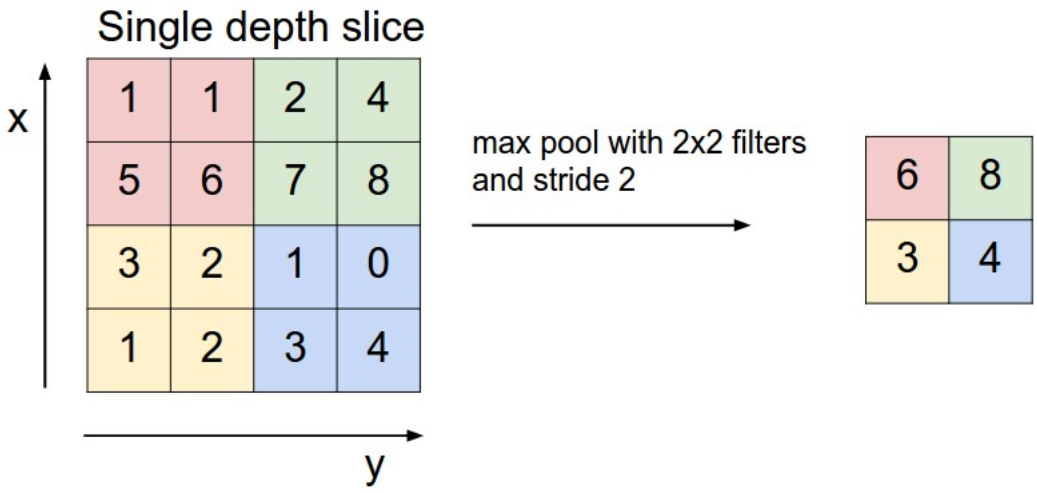

Figure 2.7: Example of max pooling operation Karpathy (2017)

Figure 2.7 presents a max pool with a 2x2 filter size, and a stride of 2, meaning that 2x2 pixels are compared and that the sliding window moves 2 pixels for each comparison. I practice this means that the 75% of the activations from the previous layer is discarded.

2.3 Height estimation using remote sensing

There are many different ways of estimating heights using satellite data such as SAR and multispectral imagery. This section will give the theoretical background for some of the most commonly used techniques.

2.3.1 Synthetic Aperture Radar (SAR)

The first technique involves using a Synthetic Aperture Radar on a moving platform, in this case a satellite. By sequentially transmitting electromagnetic waves onto the earth's surface and collecting the reflected echoes, the SAR satellites can collect high-precision, 3-dimensional data.

One of the key advantages of the SAR satellites is that they take advantage of the fact that they are moving quickly. Since the transmission and reception occur at different times, the platform

has moved, thus creating a synthetic aperture that is much larger than the satellite antenna (see Figure 2.8).

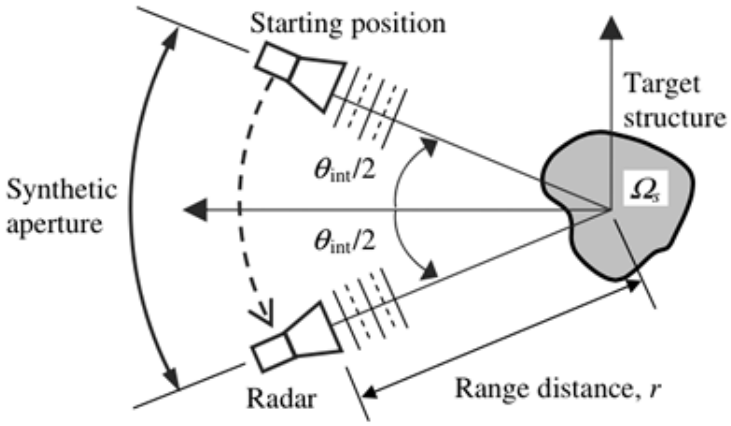

Figure 2.8: Concept of syntetic aperture **?**

The technique provides a finer spatial resolution to the collected data, making it possible to do height estimations with a sub-decimeter accuracy.

Interferometric synthetic aperture radar (InSAR)

While SAR makes use of amplitude and absolute phase of the returned signal, InSAR use a differential phase of the reflected signal, represented in what is called a phase image.

Looking at a phase image completely isolated will not prove very useful, as it would appear visually random. This is because, in practice, the phase of the return signal is affected by a lot of different factors, resulting in no apparent correlation between the pixels in the image.

To get useful information these phase images, some of the factors discussed above have to be removed. The process of doing so is referred to as interferometry, and it uses two phase images taken from the same position to generate an interferogram (see Figure 2.9).

Producing an inferiogram consists of multiple steps:

Co-registration Using a correlation function the two images are co-registered by finding the offset and difference in geometry between them.

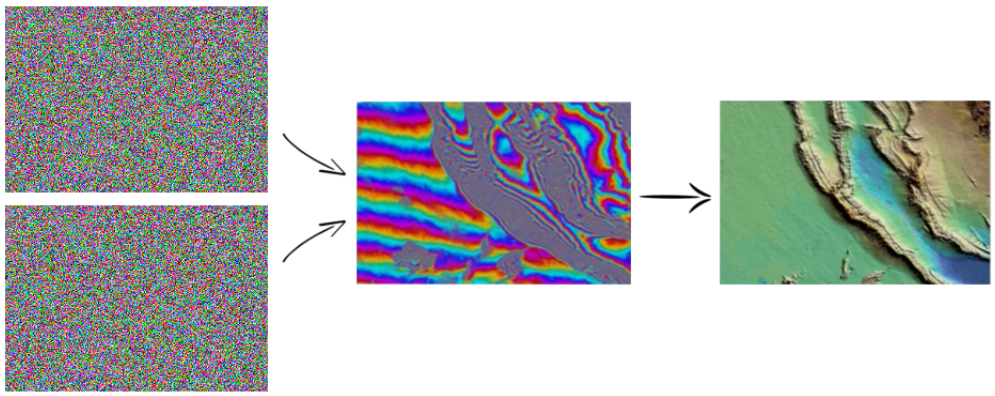

Figure 2.9: Generating an interferogram

Re-sampling In the re-sampling step, one of the images (referred to as the slave) is re-sampled to match the geometry of the other (called the master). What this means in practice is that each pixel represents the same area of ground in both images.

Cross-multiplication and flattening After re-sampling the images the inferiogram is generated by taking the cross product of each pixel, and the interferometric phase due to the curvature of the earth is removed (flattening).

Filtering Lastly, it is common to filter the basic inferiogram to amplify the phase signal and to interpolate over phase jumps to produce a continuous deformation field.

Can be used both to generate high precision digital elevation models by having two satellites record data synchronously and to measure height differences over a period very accurately.

2.3.2 Height detection using shadows from imagery

For height estimation of specific objects, shadow estimations can be applied. This technique uses a high-resolution image, as well as knowledge about the position of the sun, the location of the image projection center and the length of the projected shadow to estimate an object's height (Figure 2.10).

Looking at Figure 2.10 the height of the object can be found by:

$$tan(\mu) = \frac{H_{object}}{L_{shadow}} \quad \Rightarrow \quad L_{shadow} = \frac{H_{object}}{tan(\mu)} \tag{2.7}$$

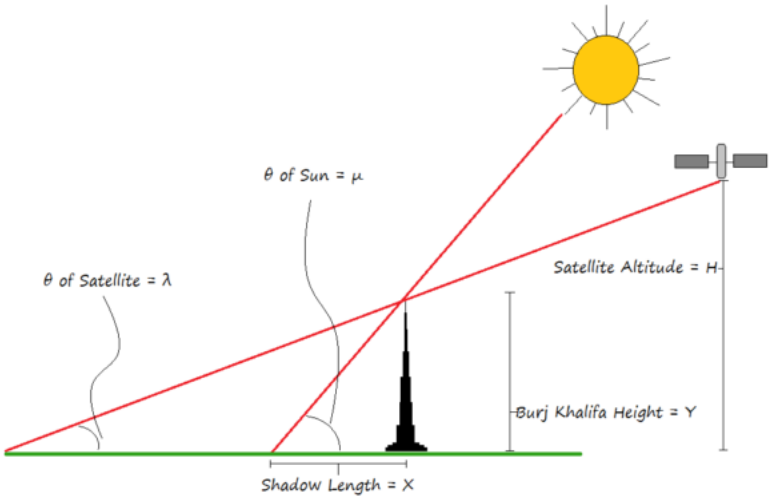

Figure 2.10: Height estimation of Burj Khalifa using shadow estimation (GISLounge, 2014)

Since the satellite image rarely is taken with the projection center directly above the object (nadir angle = 0°), the blocked length of the shadow has to be estimated. Since the height of the object is the unknown, estimating the blocked length of the shadow is an iterative process, where a new calculated, temporary value for the height is used in each iteration. Calculating the length of the blocked shadow is also very straightforward:

$$tan(90-\lambda) = \frac{L_{blockedshadow}}{H_{object}} \quad \Rightarrow \quad L_{blockedshadow} = H_{object} * tan(90-\lambda) \tag{2.8}$$

In Equation 2.8 90-λ defined as the Off-nadir angle.

It is important to remember that if this technique shall produce exact results, some parameters has to be known in the moment of the capture:

- The position of the satellite
- The time
- The position of the object with the unknown height

Chapter 3

Related Work

3.1 Standard methods for shape detection

Before looking at the use of neural networks for shape recognition in images, some more standard approaches are presented.

3.1.1 Shape detection using the Hough Transform

Shape detection and feature extraction in images, using Hough Transforms has been a subject of research for many years. The algorithm was first popularized in computer vision in 1981 by Ballard (1981) which applied a generalized version of the algorithm to detect of curves in grayscale images.

The article describes how boundary detection plays a crucial role for feature extraction in images, and how a generalized Hough algorithm can use edge information to define a mapping from the orientation of an edge point to a reference point related to the shape.

3.1.2 Simple Linear Iterative Clustering (SLIC)

Achanta et al. (2012) proposes a superpixel-segmentation algorithm (SLIC), which in their opinion is best suited to meet these demands. They compare their algorithm to a variety of state-of-the-art superpixel methods and conclude that none of the existing techniques are satisfactory in regards to the points.

The SLIC algorithm is relatively simple to understand. One of its fundamental principles is that, by limiting the search space for each cluster center (points in the regular raster grid), it reduces the search speed significantly. This is achievable due to the fact that one of the primary goals of the algorithm is to create a set of approximately equal-sized superpixels. Thus, instead of searching the whole raster grid for each cluster center, the algorithm only has to search for edge pixels at a distance equal to D, as shown in Equation 3.1.

$$D' = \sqrt{\left(\frac{d_c}{m}\right)^2 + \left(\frac{d_s}{S}\right)^2} \tag{3.1}$$

In Equation 3.1 d_c is the Euclidean distance between two pixels in terms of color and d_s is the pixels euclidean, spatial distance. Furthermore, S is the sampling interval of the cluster centers ($S = \sqrt{N/k}$, where N is the number of pixels in the grid and k is the desired number of superpixels) and m is a fixed constant based on the color diversity in the image.

Since the algorithm generates superpixels by clustering pixels based on their color and spatial proximity, creating a five-dimensional, *labxy* space, one would think that the distance could be found by simply taking the 5D Euclidean distance. However, it turns out that for large superpixels, spatial distance outweighs the color proximity. Which is why the two distances d_c and d_s are weighted.

3.2 The development of Convolutional neural networks

Since McCulloch and Pitts created what is acknowledged as the first neural network in 1943, using simple electrical circuits (Mcculloch and Pitts, 1943), they have played an essential role in the field of pattern recognition.

Since the late 1990's the idea of using convolutional operations in these networks has been considered more and more prominent (Le Cun et al., 1998), and this approach is still one of the leading research fields within ANN research (Wu et al., 2017). This section will discuss the development of the convolutional neural networks the last two decades.

3.2.1 Early adaption of convolutional neural networks

The earliest attempts of using convolutional operations for pattern and object recognition in neural networks was first made nearly twenty years ago by Le Cun et al. (1998). In the paper, a convolutional neural network is used to analyze handwritten characters.

3.2.2 Deep Convolutional Neural Networks

It was, however, not until Alex Krizhevsky, Geoffrey Hinton, and Ilya Sutskever won the ImageNet [1] 2012 competition (ILSVRC'12), that CNN's became acknowledged as one of the most sophisticated approaches for image recognition. Their deep convolutional neural network (commonly called AlexNet) consisted of five convolutional layers, each followed by a pooling layer (max-pooling), and three fully-connected softmax layers (Krizhevsky et al., 2012). The network applied two different methods; Data Augmentation and Dropout layers, to reduce overfitting.

Even though the AlexNet was a significant breakthrough for the convolutional neural networks, it was criticized for not presenting a good ground for understanding what was happening inside the network, thus making it hard to improve. One of the solutions to this problem is the ZF Net, which applies deconvolutional neural networks (Zeiler et al., 2011) to map the dense feature space produced by a CNN back to its original pixel space (Zeiler and Fergus, 2013). Figure 3.1 shown how a deconvolutional network can help visualizing the feature space of a CNN.

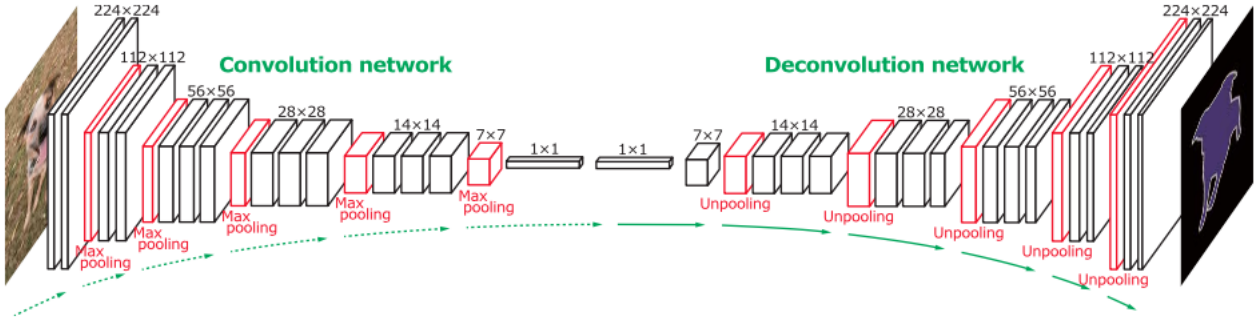

Figure 3.1: Process of visualizing the feature space of a CNN (Noh et al., 2015)

To do so, the ZF Net successfully unpool, rectify and filter the feature map, generated by the CNN, to reconstruct the activity inside the network.

Unpooling In general, the max-pooling operation is non-reversible, since there are no tracking of the positions of the selected features, as seen in section 2.2.7. Therefore, to reconstruct the feature map, the location of each selected maxima had to be stored.

Rectification Their CNN used the common ReLU activation function for each Convolution Layer. Therefore the reconstruction layers also need to use this activation function to prevent negative values.

[1] ImageNet is a very large dataset consisting of 15 million labeled, high-resolution images divided into over 22.000 categories.

Filtering Since CNN's apply kernel filters to each convolution layers input volumes, the filtering has to be inverted when reconstructing. To do so, the same filters are transposed (remember that the filters are matrices) and applied to the rectified activation maps.

GoogLeNet

Another network, whose creators have criticized the standard structure of the convolutional neural networks, is the GoogLeNet (Szegedy et al., 2014). The authors of the article claim that their network was significantly more accurate than the AlexNet, while at the same time only using one-twelfth of the parameters.

The GoogLeNet introduces what is called an inception architecture (see Figure 3.3), which the main idea is to cluster neurons in the network which have highly correlated outputs. This is because, in images, the correlation between pixels tend to be local.

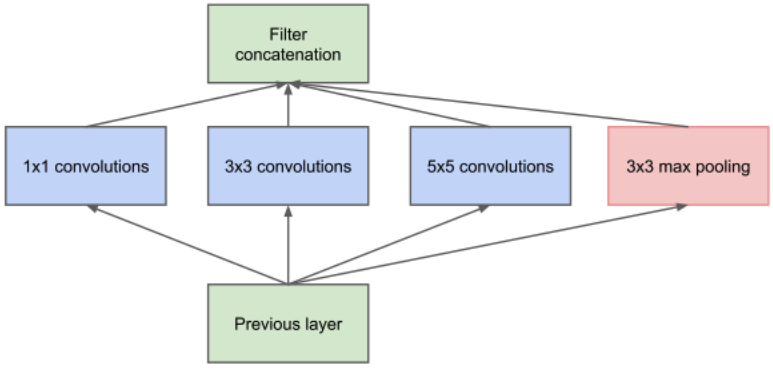

(a) Inception module, naïve version

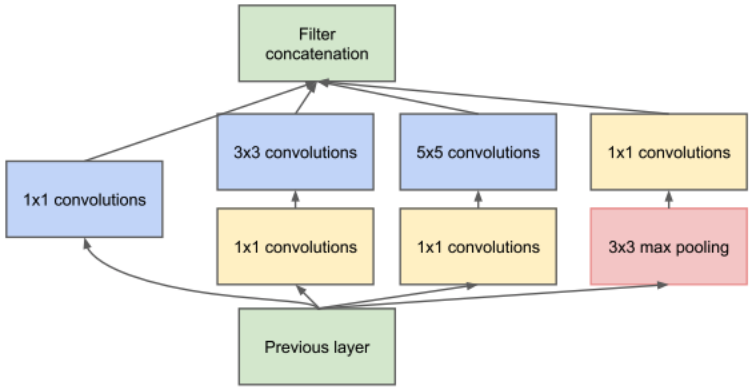

(b) Inception module with dimensionality reduction

Figure 3.2: Two versions of the inception module (Szegedy et al., 2014)

The basic structure of the inception module is to do multiple convolution operations, in parallel,

with different sized filters, and then concatenate the results before passing them on to the next layer. Additionally, a parallel pooling operation is added to each inception module, because such operations have proven them selfs successful in other CNN's.

The naive version of these "micro-networks" is shown in Figure 3.3 (a). One issue with this naive version is that, even with a modest number of 5x5 convolutions, the computational cost can be quite expensive. This is solved by keeping the representation of the information as sparse as possible, and only compress the signals when they have to be aggregated. To do so, 1x1 convolutions are used to compute reductions before the 3x3 and 5x5 convolutional operations are applied (Figure 3.3 (b)).

VGGNet

Another example of a successful deep convolutional neural network is the VGGNet. This network does not present any new concepts, but the authors argue that by stacking multiple layers, doing small convolutional operations (3x3 and a few 1x1) they can outperform the other discussed networks (Simonyan and Zisserman, 2014).

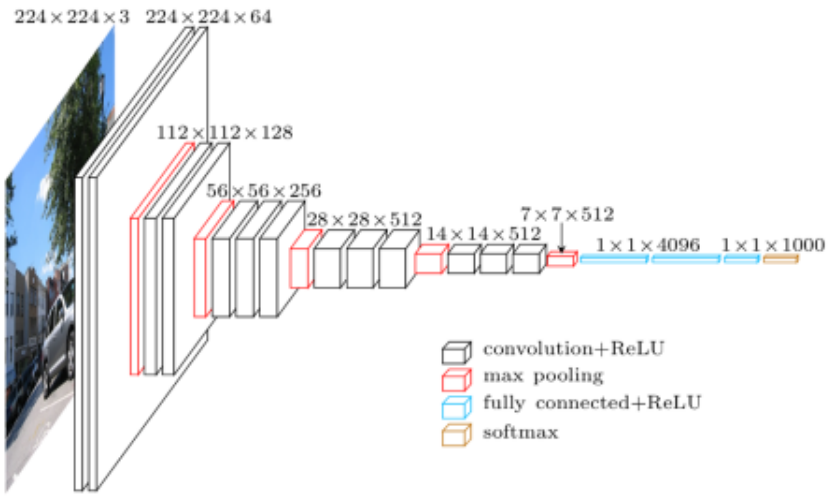

Figure 3.3: The 16-layer VGGNet (Frossard, 2016)

An important difference between this network and previous networks is that the creators focus on depth, thus calling the network a very deep convolutional network.

ResNet

A problem that arises with deeper convolutional neural networks is the degradation problem. As depth increases in the network, the accuracy decreases (Figure 3.4).

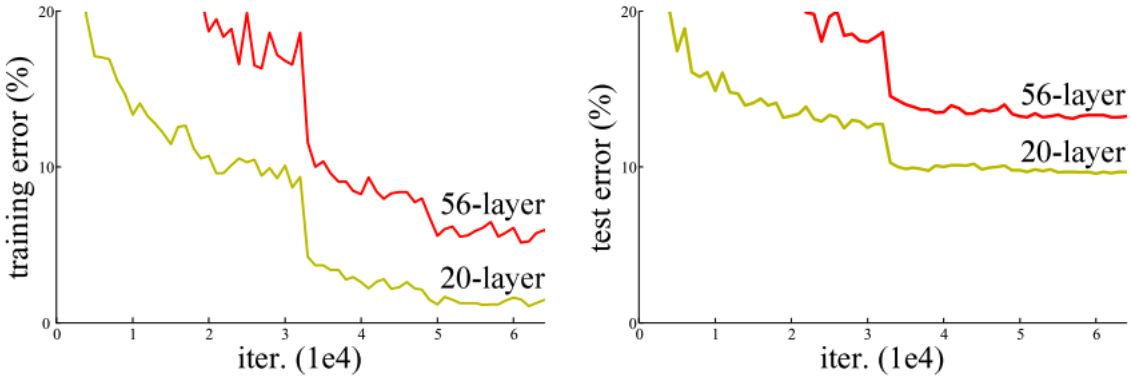

Figure 3.4: Degradation problem (Wu et al., 2017)

Surprisingly enough this decrease in accuracy is not due to overfitting, as adding more layers effects the training error as well (Wu et al., 2017). In theory, any deep network should be able to perform at least as good as a shallower network, only by seeing the layers that differentiate the two networks as identity mappings.[2] This, however, does not seem to be the case in practice, suggesting that networks have problems learning identity mappings by multiple, non-linear layers.

To solve the degradation problem, the authors of the paper introduces two new concepts, which sets the foundation for their residual neural network (ResNet).

Residual mapping The paper hypothesizes that it is easier to optimize residual mapping, thus introducing the residual mapping function:

$$F(x) := H(x) - x \tag{3.2}$$

where H(x) is the desired, underlying mapping function after 2 weight layers.

Shortcut connections Connections which skip one or more layers, as seen in Figure 3.5, in order to obtain the desired mapping function H(x).

Using these concepts, the authors were able to create the winning 152-layer deep ResNet of the ILSVRC'15.

[2]The map which assigns every member of a set A to the same element id_A. It is the same as the identity function: $id(x) = x$

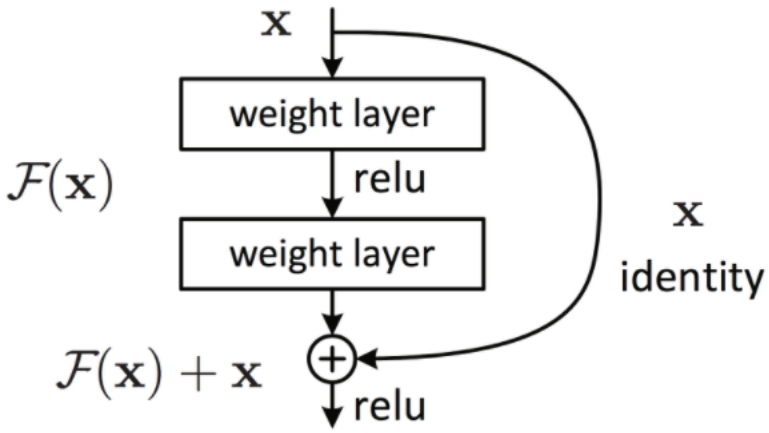

Figure 3.5: A residual building block (Wu et al., 2017)

3.3 Semantic segmentation using convolution neural networks

In later years there has been significant progress in the field of edge detection in imagery has been made due to advances in deep learning (Yu et al., 2017). Marmanis et al. (2016) present an end-to-end semantic segmentation method for segmentation in aerial images of the ISPRS semantic labeling dataset [3]. Using a Fully Convolutional Network and Conditional Random Fields, they can do a per-pixel semantic segmentation of a very high-resolution aerial image with an accuracy of 88.5% based on five different classes.

Furthermore, Kaiser et al. (2017) present a solution, which deals with the lack of labeled training data available. To do so, the authors make use of the open-source map data library OpenStreetMap, to automatically derive weakly labeled training data. By matching this data with aerial imagery from Google Maps, and training a fully convolutional neural network, they are able to classify buildings and roads at a high level of accuracy (see Figure 3.6).

Other attempts for semantic segmentation in remote sensing have been made with different variants of deep convolutional neural networks (Kemker et al., 2017). In their paper, they propose an approach for using the Digital Imaging and Remote Sensing Image Generation (DIRSIG) modeling software to generate a large quantity of synthetic multispectral imagery and corresponding labels. For the semantic segmentation, the authors adapt two fully-convolutional neural networks called SharpMask (Pinheiro et al., 2016) and RefineNet (Lin et al., 2016). Their results show that it is possible to use synthetic imagery to assist the training of semantic segmentation networks when there is not enough annotated image data.

[3] Link: http://www2.isprs.org/commissions/comm3/wg4/semantic-labeling.html

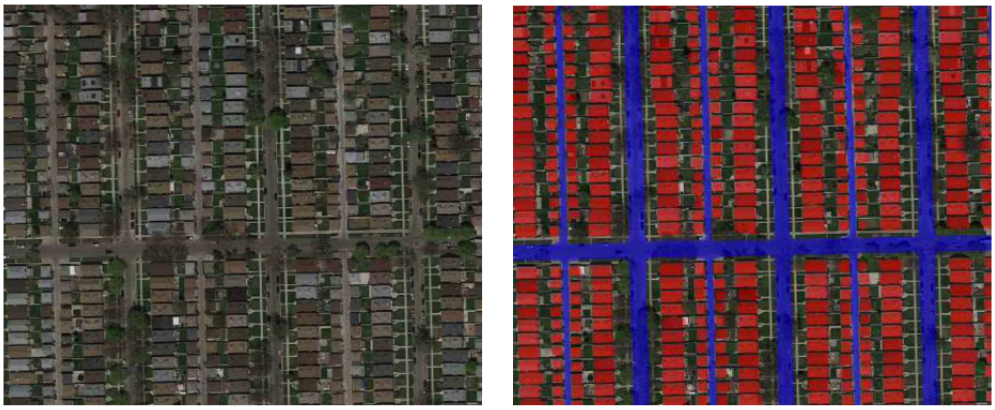

Figure 3.6: Results from classification of buildings and roads (Kaiser et al., 2017)

3.4 Height estimation form a nadir perspective

As seen in section 2.3 there are many different techniques that can be applied to estimate the height of a building. This section will focus on different attempts to retrieve height data, using satellite imagery.

3.4.1 Building height retrieval from VHR SAR Imagery

After the launch of TerraSAR-X in 2007, a satellite that was designed to acquire high-resolution X-band radar images of the entire planet, it was possible to gather SAR data with a resolution of down to 1 meter (Airbus, 2017). In contrast to other optical, spaceborne sensors, such as Ikonos, Quickbird, and WorldView, satellites using SAR overcome the difficulties of weather conditions and lack of sun illumination.

Using the SAR images provided by the satellite Brunner et al. (2008) was able to estimate the height of man-made structures with a sub-meter precision by automatically reconstruct 3-D models, using a "hypothesis generation-rendering-matching" procedure. The basic principle was that using an optimization algorithm, the height of a building is found by testing different height hypothesis against a single SAR image. The estimation is done without modeling its exact radiometry since this would require extensive apriori knowledge about the roughness parameters and dielectric constants of the surfaces. Generating this height model becomes an optimization problem Equation 3.3.

$$\hat{h} = \underset{h,\vec{s}}{argmax} \left\{ M \left[\hat{X}_{\vec{s}}(\vec{H}), X \right] \right\} \tag{3.3}$$

In Equation 3.3 X is the true SAR image, $\hat{X}$ is the simulated SAR image at height h, M is the matching function, and $\vec{H}$ is the simulated hypothesis.

Brunner et al. (2008) tested their method on different types of buildings, where flat buildings gave a mean accuracy of $0.3 \pm 2.1m$.

3.4.2 Height estimation from InSAR analysis

Another approach for height detection using SAR satellites, is interferometric SAR (InSAR) analysis, as attempted by Liu et al. (2015). In their paper, they used images taken on December 5 and 27, 2007 to generate an interferogram over San Francisco. The technique was based on extracting potential layover areas from the interferogram and use these areas to measure the height of the buildings using the relationship between the height of an object and the layover observed in the interferogram (Equation 3.4).

$$\Delta\Phi = \frac{4\pi B_N}{\lambda H sin\theta}\Delta R \tag{3.4}$$

In Equation 3.4 $\Delta\Phi$ is the phase difference within one pixel in the layover area, B_N is the perpendicular baseline distance, λ is the radar wavelength, H is the satellite altitude, and θ is the angle of incidence (see Figure 3.7).

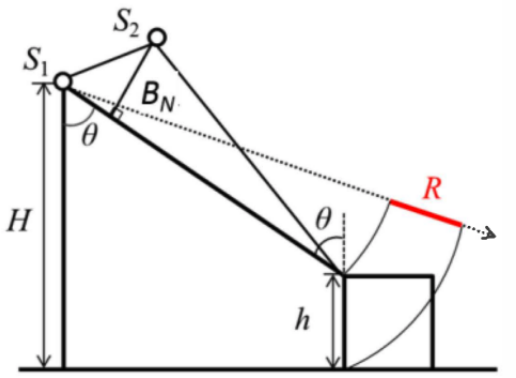

Figure 3.7: A schematic image of geometrical characteristics for a building in a slant-range SAR image (Liu et al., 2015)

Using this method Liu et al. (2015) were able to estimate the height of high-rise buildings in a crowded area with a RMS of 13m and an average difference between detected results and the reference values of 6.6m.

3.4.3 Height estimation using shadow measurement

While some height extraction methods require precise specifications regarding the geometrical properties of remotely sensed data, Comber et al. (2012) present a method for determining height using building shadows. By classifying buildings and their associated shadows based on a series of different measures (see Figure 3.8), and applying Equation 3.5 the authors were able to give relative good height estimations.

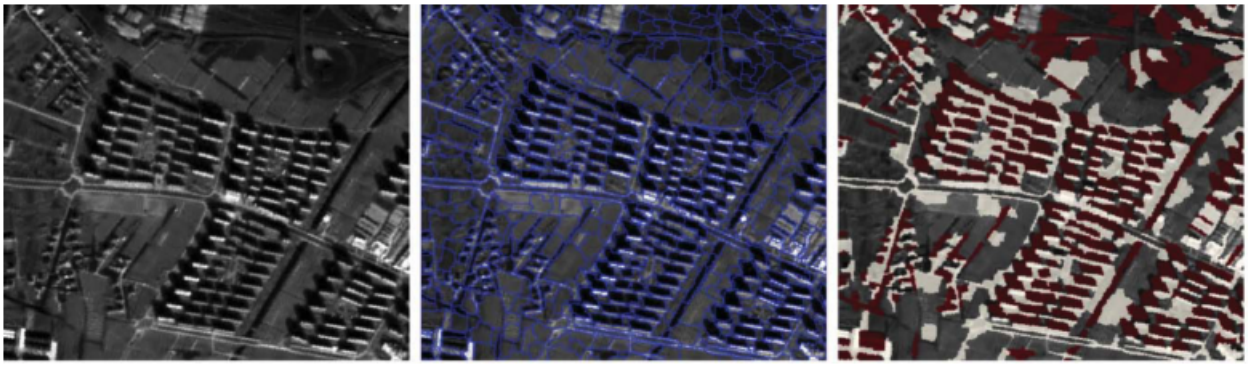

Figure 3.8: Classification of buildings and their assiciated shadows (Comber et al., 2012)

$$H = \frac{W}{\frac{cos(\phi_{sun}+90+\phi_{az})}{tan(\phi_{sun})}} \tag{3.5}$$

Other attempts have also been made regarding estimation heights using shadows, such as Shao et al. (2011) who addresses the issue of distinguishing between shadows and water in aerial photographs. In their approach, they merged the two classes into a single shadow/water class and used different spatial indices such as object size, shape, and spatial neighbor information to separate shadow and water. They further used a standard trigonometrical approach to estimate the building heights. Their results can be seen in Figure 3.9.

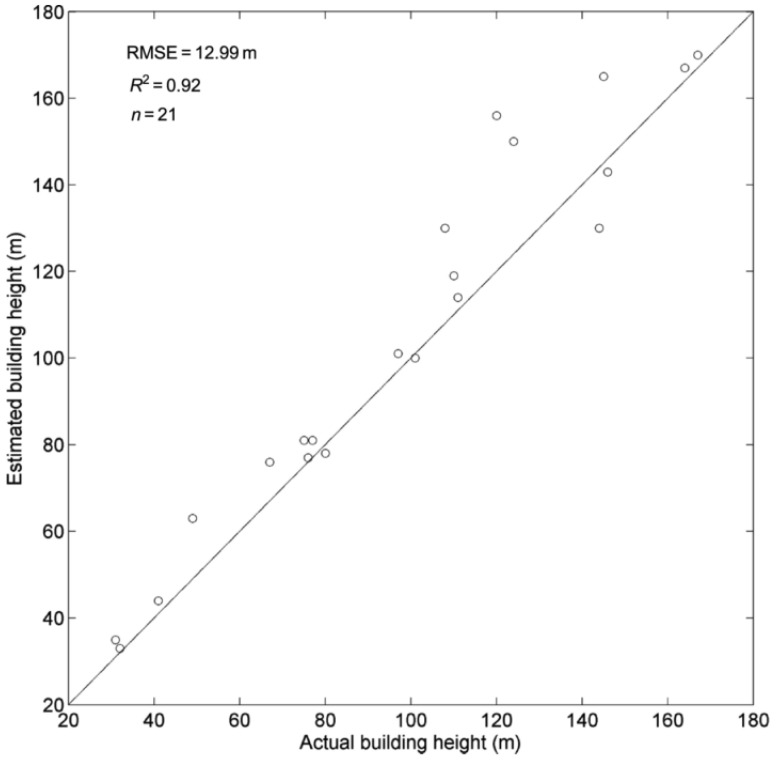

Figure 3.9: Accuracy evaluation of building height estimation (Shao et al., 2011)

Chapter 4

Evaluating the methods

There are evidently a large variety of different methods available for solving the task at hand. Based on the work done in the previous chapter, this section of the paper will discuss possible solutions to the problem.

4.1 Available data

One important aspect that should be considered is the amount of data available for the different methods. A key criterion for the success is that there exist satellite constellations that can provide frequently updated image data over the requested area. New images should be available on a weekly basis, and the resolution of the images has to be approximately one meter or less for the results to be accurate enough.

Multispectral images

There are many different satellite constellations that provide frequently updated multispectral imagery of the requested area, such as the Sentinel-2 (ESA), SkySat (Planet, 2017), and WorldView (DigitalGlobe, 2017) satellite constellations. All three constellations have a sub week revisit time over any point on earth. However, the ground sampling distance (GSD) varies with a factor of more than ten.

While both SkySat and WorldView provide a submeter accuracy on their images, the Sentinel-1 constellation has an expected GSD of 10x10 meters, which will not be sufficient for shadow measurements. Furthermore, it has to be taken into consideration that while data provided from the Sentinel constellations are free of charge, data from both SkySat and WorldView comes

at a certain cost. Data provided by the Sentinel-2 constellation might, however, be accurate enough to locate the oil tanks.

A general issue with multispectral images is that they are sensitive to cloudy weather and daylight. This can pose as an issue if the system is expected to continuously provide data without deviations.

Radar images

Another type of images that are not affected by clouds or the time of day is radar images. In terms of radar-based methods, there are also a lot of satellite constellations that can be of interest. For example, while Sentinel-2 provide multispectral images, the Sentinel-1 constellation provides radar-images with resolutions down to 5x5 meters (ESA).

Other constellations, such as the TerraSAR-X can provide even higher resolutions as low as 1 meter, and the revisit time of the TerraSAR-X constellation has a revisit time of 11 days (**?**).

4.2 Amount of data required for analysis

An essential difference between the different methods presented in the previous sections is the amount of data needed to provide an accurate analysis. For example, simple image segmentation can be done in a single image using Simple Linear Iterative Clustering (Achanta et al., 2012) as seen in Figure 4.1. Furthermore, by knowing the approximate size of the oil tanks, a general Hough Transform (Ballard, 1981) can be used to detect their circular shapes as seen in Figure 4.2. Image segmentation and shape detection using machine learning based methods require large amounts of training examples, which can be very hard to acquire. But as seen in Kaiser et al. (2017) and Kemker et al. (2017) it might be possible to automatically collect and label training data.

Advanced methods in machine learning, such as Convolutional Neural Networks, have proven themselves as very efficient in image segmentation, but also in terms of classifying the different segments and even associating values with them if given the correct training data. This means that by acquiring the right training data, which in this setting would be the actual inventory of an oil tank at a specific time, and relate these values to aerial photographs of the same tanks, it would be possible to train a network into doing the actual inventory estimation directly.

When it comes to height estimation using radar images, Brunner et al. (2008) presented a method that only acquired a single radar image to estimate the height of buildings using the SAR prin-

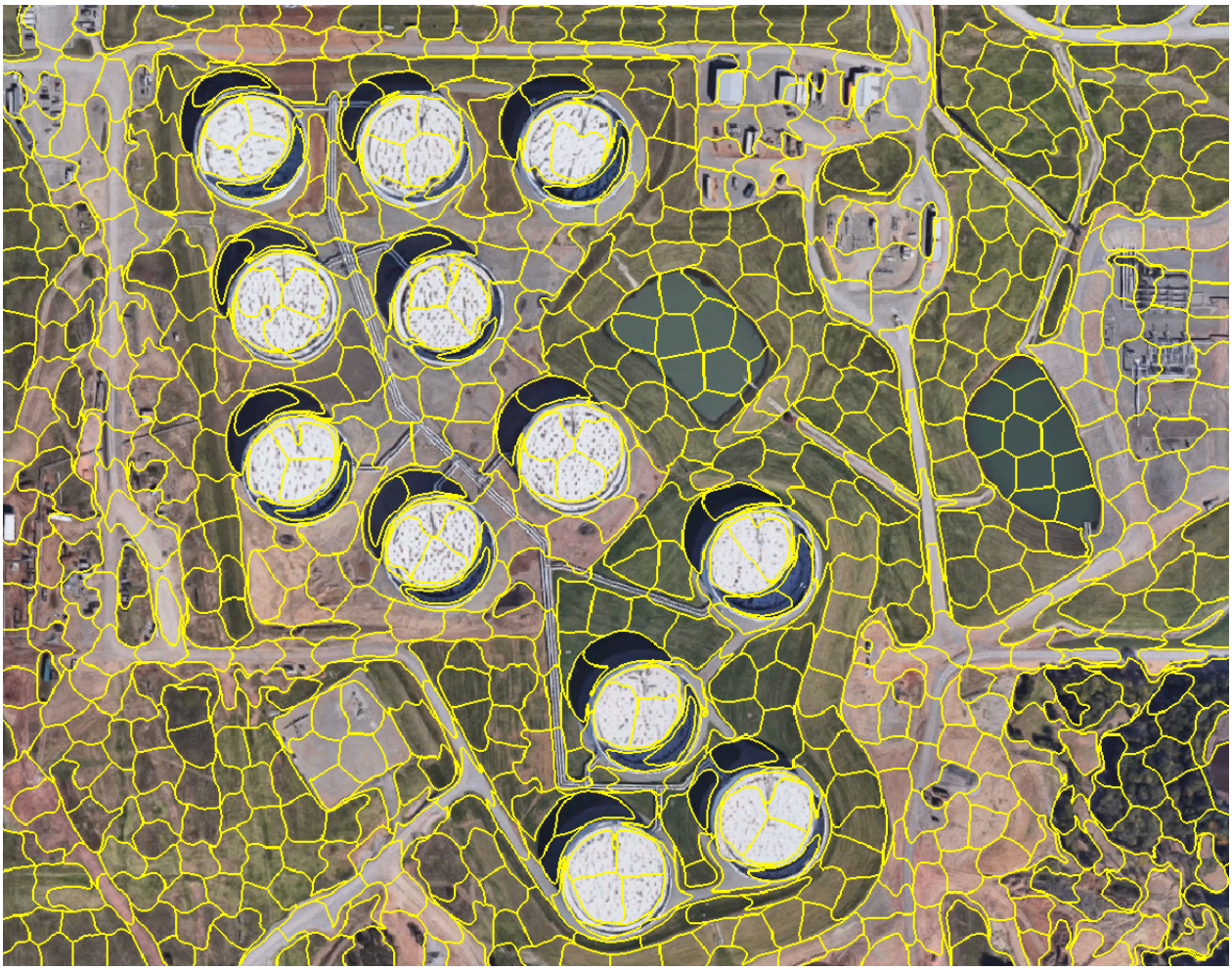

Figure 4.1: Simple implementation of SLIC superpixel segmentation on image taken from Google Earth

ciple. To generate an interferogram, two-phase images are required as explained in Liu et al. (2015). Furthermore, height estimation using shadow measurement can also be done using single, multispectral images as shown by Comber et al. (2012) and Shao et al. (2011).

4.3 Choosing a method

By taking the above comparison into consideration, it becomes clear that regarding pure circle detection, the generalized Hough transform stands out as the most efficient method. The fact that we have pre-knowledge about the shape of the objects we are trying to locate makes it much easier to use a standard approach. However, the generalized Hough transform will, isolated, not be able to estimate any heights, and would have to be combined with another method for height

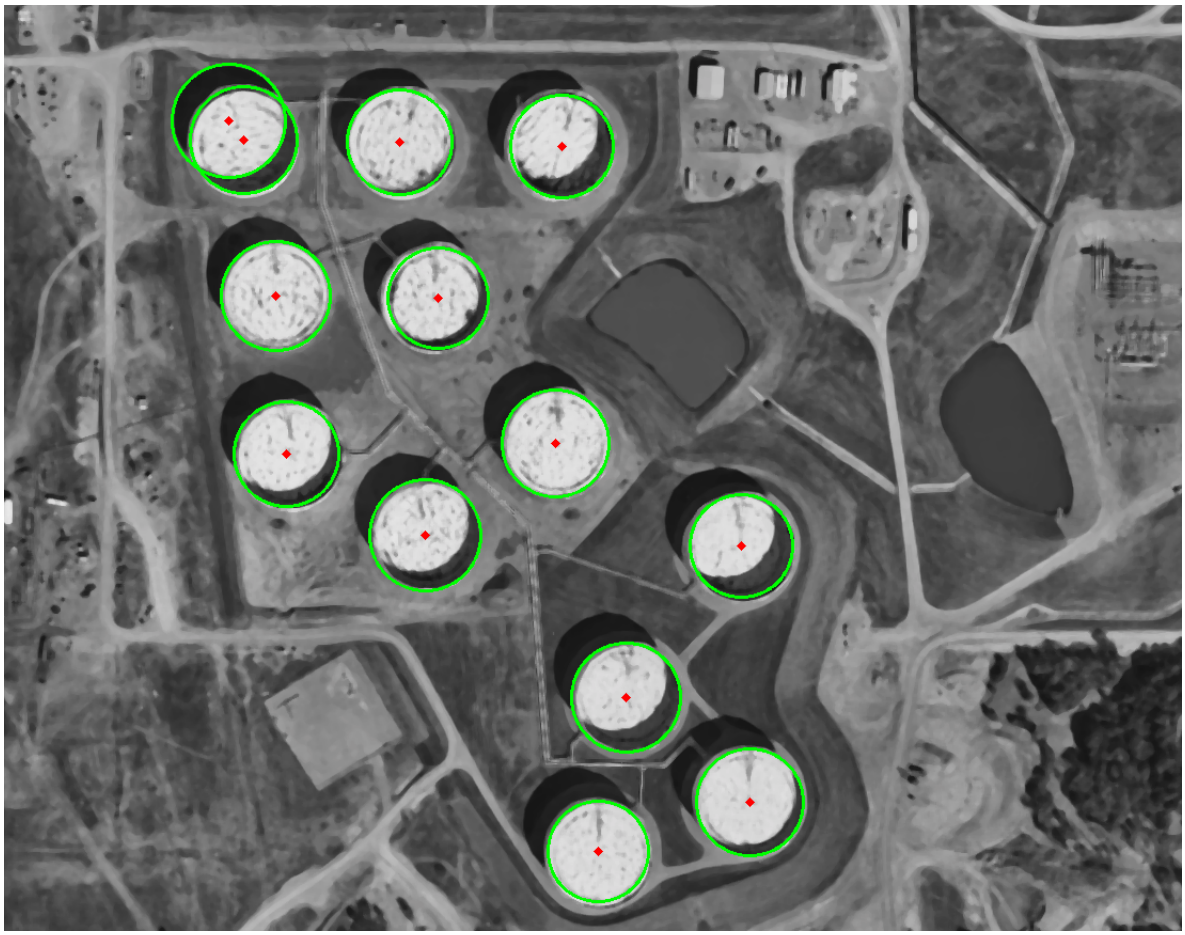

Figure 4.2: Detecting circles of similar size in an image taken from Google Earth using a generalized hough transform

estimation. By looking at Figure 4.2, height estimation using shadow measurements might be the best approach. This is because the green circles limit the search area in terms of locating shadows since we are only interested in the shadow that is cast inside the tanks.

An important issue regarding the generalized Hough transform is the fact that if the tanks vary in size, it might not be able to find all of them, as seen in Figure 4.3.

Looking at Figure 4.1 it seems like the SLIC algorithm has potential when it comes to image segmentation as well, but an issue is that it is hard to extract the correct edges without any prior knowledge. And the same issue regarding height estimation arises since the algorithm will have to be combined with another method.

As previously stated, it has been shown that convolutional neural networks outperform the state-of-the-art methods for image segmentation in terms of accuracy, if they are provided with enough good training examples. There are several ways to acquire training data, such as automatically extract training examples from OpenStreetMap as described by Kaiser et al. (2017).

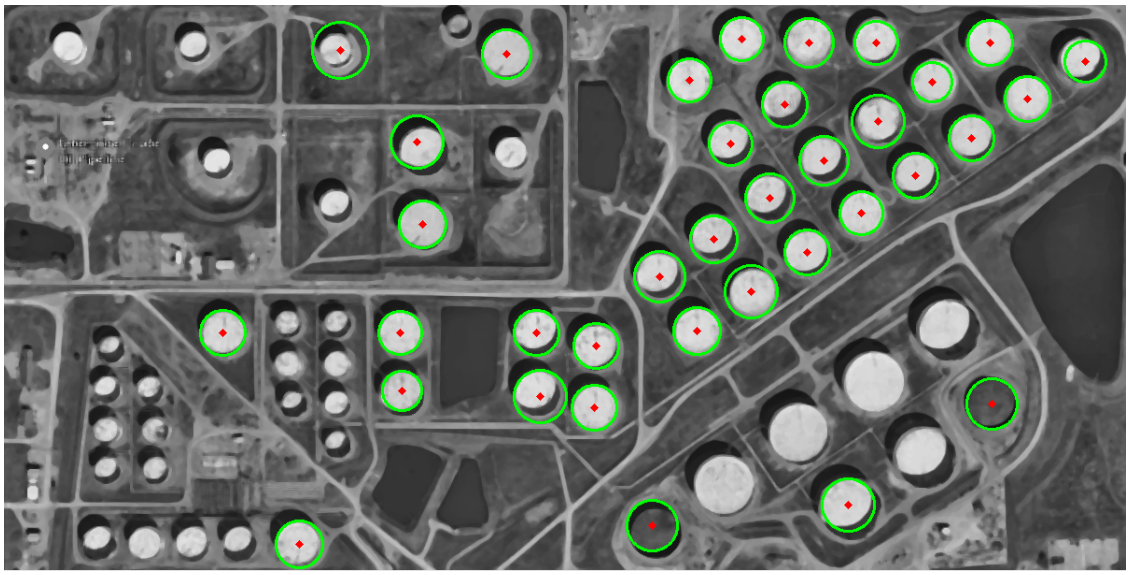

Figure 4.3: Detecting circles of different size in an image taken from Google Earth using a generalized hough transform

Since 2012 convolutional networks have been the leading method for object recognition and image segmentation (Krizhevsky et al., 2012). Furthermore, very deep convolutional neural networks such as the ResNet (Wu et al., 2017) have shown an incredible ability to create very complex functions for image analysis. The potential of these networks have yet not been fully explored, and there are still many applications that have not been discovered. One of them being building height extraction from aerial imagery.

By comparing the three presented methods for height estimation, it is clear that Brunner et al. (2008) presented the best results in terms of accuracy. However, both the relatively slow renewal time and the fact that the data can be quite challenging to acquire is something that has to be taken into account since the estimations should be done automatically at a sub-week frequency. Sentinel-1 provide this data automatically at a renewal time of 6 days, but with a less accurate resolution of 5x5 meters.

Even if Liu et al. (2015) did not achieve very high accuracy in their paper, there are still some aspects of interferometry that can be explored. The TanDEM-X mission is a mission is a public-private partnership between the German Aerospace Center and Airbus Defence and Space. The mission uses the TerraSAR-X and the TanDEM-X satellite to generate a high precision DEM, covering the whole planet. However, this DEM would have a renewal time of 11 days, which is, unfortunately, a too long period. Furthermore, as mentioned in section 2.3.1 interferograms can also be used to measure height differences over time. The problem with this is that the height difference between in a certain point cannot be more than 2.5 cm between two measurements, which would not be the case in terms of the height difference of the tank roof.

After comparing the different methods, it has become clear that there are many ways to attack the presented problem. Below two different methods are presented as potential approaches to solving the problem:

- Direct estimation of the tanks inventory from shadow measurements in multispectral images, using a modified ResNet.
- Using a generalized Hough transform for tank detection, thus limiting the shadow search space, and then applying a modified ResNet for estimating a single tanks inventory in multispectral images.

4.4 Implementation

For the these methods to be tested, some aspects of implementation have to be considered. The main aspects are, what technology is needed to build the convolutional neural network and how can the data be acquired in order to train them.

Libraries for deep learning

As a result of the vast development within the field of machine learning and especially neural networks, a lot of useful tools have been developed to aid the researchers in making it easier to implement new architectures. Two of these tools are Tensorflow and Keras.

Tensorflow Tensorflow is an open source software library used for dataflow programming, and it is very much used for machine learning applications such as neural networks. Tensorflow was developed by the Google Brain team for internal use at Google but was later released under the Apache 2.0 open source license[1] in 2015.

Keras Keras is an open source neural network library written in Python designed to enable fast experimentation with deep neural networks. The library runs on top of Tensorflow and contains numerous implementations of commonly used neural network building blocks.

By using these libraries in further research, it will be possible to test many different implementations of different networks, modify them and compare them with each other.

[1] Link: https://www.apache.org/licenses/LICENSE-2.0

Gathering Data

For a neural network to generalize beyond its training examples, it has to be provided with a substantial amount of labeled data. For example, the GoogleNet was trained on 1.2 million images when winning the ILSVRC 2014 challenge (Szegedy et al., 2014). However, the amount of data required for training varies based on the task at hand. Wu et al. (2017) did an analysis based on the CIFAR-10 dataset, which consists of 50.000 training and 10.000 test images divided into 10different classes. By training their ResNet-110existthey achieved an accuracy of 6.43%.

Of course, 50.000 training examples are still a lot of data, but it is substantially less than 1.2 million training examples. Fortunately, it turns out that CNN's are good at transferring learning. Meaning that once a network has been trained with an extensive database, it has adapted well enough to the structure of image data in general so that it can be adapted for a new task with relatively little training (Marmanis et al., 2016).

There are several ways to attack the presented problem in terms of gathering enough data. Firstly, historical (as detailed as possible) of the inventory at Cushing has to be provided. There are many sources for this data, such as the U.Ss Energy information Administration which provides weekly, historical data back to 2004 of the total inventory.

Furthermore, this data has to be linked to time-stamped, high-resolution satellite images over the area. This might become a problem for the earlier parts of the inventory data, but satellite data providers such as Digital Globe and Planet Labs large achieves which reach back many years.

Another approach is to train the network on something other than oil tanks, and then seeing how the network performs when trying to estimate the height difference between the tank walls and the roof. For example, it would be much simpler to train the network on trying to determine the height of buildings. This is because there exist large amounts of detailed building height models that can be combined with time-stamped, satellite images over areas that the height models represent. By combining these data sets, a significant amount of labeled training data can be generated.

Chapter 5

Conclusions, Discussion, and Recommendations for Further Work

Many attempts have been made in terms of semantic segmentation, and advances are still being made.

5.1 Summary and Conclusions

In this paper, we have been investigating different approaches to estimate the total inventory of the famous price settlement point for West Texas Intermediate of the New York Mercantile Exchange in Cushing, Oklahoma. To do so, two different problems have been identified, which is locating the oil tanks in from an aerial image and estimating the inventory based on the height of the tanks floating roofs.

First, the theoretical background for different methods is presented, including standard approaches for semantic segmentation, theory related to artificial neural networks, height estimation using SAR and InSAR analysis and trigonometrical height estimation using building shadows cast by the sun.

Furthermore, related work for the different theoretical subjects is presented. The primary purpose of this chapter is to give an understanding of what has been done so far, and where the technology is today.

Then the different methods are compared, evaluated and combined to come up with solutions that are suitable for the task at hand. Two different approaches were selected as most suitable; Direct estimation of the tanks inventory from shadow measurements using a modified reset and

using a generalized Hough transform for tank detection, thus limiting the shadow search space, and then applying a modified ResNet for estimating a single tanks inventory.

Lastly, the implementation of the method is discussed by presenting some tools that enable fast experimentation with deep neural networks and different approaches related to requiring enough training data is discussed.

There exists an extensive amount of different techniques for both aerial image segmentation and height estimation from remote sensing. In the last five years, convolutional neural have played a crucial role in the development of image segmentation methods, but their applications reach far beyond this particular field. In this paper both traditional and machine learning based methods have been explored through theory and related work. Using this knowledge two methods has been evaluated as the most plausible approached to retrieve an accurate and frequently updated estimate of the total oil inventory in the tanks located in Cushing, Oklahoma.

For further work, these methods should be implemented and tested to determine if it is possible to do precise enough estimations. If so, there would lie a great economic potential in these numbers because of Cushing's importance as a price settling point for West Texas Intermediate of the New York Mercantile Exchange.

5.2 Discussion

The two methods selected as potential solutions in this paper are chosen because they present the largest likelihood of solving the specific problem presented. The decision is based on the availability of frequently updated satellite data and a certain level of accuracy. This being said, there lies a huge potential in information extraction from frequently updated remote sensing data that could benefit from the other methods presented in this paper. Especially methods within the field of machine learning could be interesting because of their ability to generalize beyond the data they have been trained on.

With new satellite technology being developed every year providing open, updated data at increasing frequencies, it is important to develop methods that can derive, process and analyze these methods automatically. Hopefully, this article can provide some insight as to what exists and how they can be taken advantage of in any further research.

Bibliography

Achanta, R., Shaji, A., Smith, K., Lucchi, A., Fua, P., and Süsstrunk, S. (2012). SLIC superpixels compared to state-of-the-art superpixel methods. *IEEE Transactions on Pattern Analysis and Machine Intelligence*, 34(11):2274–2281.

Airbus (2017). Technical Information : TerraSAR-X.

Ballard, D. H. (1981). Generalizing the Hough Transform To Detect Arbitrary Shapes*. *Pattern Recoqnition*, 13(2):111–122.

Brunner, D., Lemoine, G., and Bruzzone, L. (2008). Building Height Retrieval From VHR SAR Imagery Based on an Iterative Simulation and Matching Technique. 7110(3):71100F–71100F–12.

Cambridge (2017). Convolutional Neural Networks with Keras.

Comber, A., Umezaki, M., Zhou, R., Ding, Y., Li, Y., Fu, H., Jiang, H., and Tewkesbury, A. (2012). Using shadows in high-resolution imagery to determine building height. *Remote Sensing Letters*, 3(7):551–556.

DigitalGlobe (2017). Our Constellation - DigitalGlobe.

ESA. Overview - Copernicus.

Esa (2009). 50 years of Earth Observation.

Fisher, R., Perkins, S., Walker, A., and Wolfard, E. (2003). Image Transforms - Hough Transform.

Frossard, D. (2016). VGG in TensorFlow.

GISLounge (2014). Measuring Object Heights from Satellite Imagery.

Kaiser, P., Wegner, J. D., Lucchi, A., Jaggi, M., Hofmann, T., Schindler, K., and Member, S. (2017). Learning Arial Image Segmentation from Online Maps. pages 1–15.

Karpathy (2017). Convolutional Neural Networks for Visual Recognition.

Kemker, R., Salvaggio, C., and Kanan, C. (2017). Algorithms for Semantic Segmentation of Multispectral Remote Sensing Imagery using Deep Learning. pages 1–45.

Krizhevsky, A., Sutskever, I., and Hinton, G. E. (2012). ImageNet Classification with Deep Convolutional Neural Networks. *Advances In Neural Information Processing Systems*, pages 1–9.

Lary, D. J. (2010). Artificial Intelligence in Geosience and Remote Sensing. *RFID Technology, Security Vulnerabilities, and Countermeasures*, pages 75–100.

Lary, D. J., Alavi, A. H., Gandomi, A. H., and Walker, A. L. (2016). Machine learning in geosciences and remote sensing. *Geoscience Frontiers*, 7(1):3–10.

Le Cun, Y., Bottou, L., Bengio, Y., and Haffner, P. (1998). Gradient-Based Learning Applied to Document Recognition.

Lin, G., Milan, A., Shen, C., and Reid, I. (2016). RefineNet: Multi-Path Refinement Networks for High-Resolution Semantic Segmentation.

Liu, W., Suzuki, K., and Yamazaki, F. (2015). Height estimation for high-rise buildings based on InSAR analysis. *2015 Joint Urban Remote Sensing Event, JURSE 2015*, (June 2010):1–4.

Marmanis, D., Wegner, J. D., Galliani, S., Schindler, K., Datcu, M., and Stilla, U. (2016). Semantic Segmentation of Aerial Images With an Ensemble of Cnns. *ISPRS Annals of Photogrammetry, Remote Sensing and Spatial Information Sciences*, III-3:473–480.

Mcculloch, W. S. and Pitts, W. (1943). A logical calculus of the ideas immanent in nervous activity. *Bulletin of Mathematical Biology*.

Minsky and Papert (1969). *Perceptrons*.

Moon, H., Chellappa, R., and Rosenfeld, A. (2002). Optimal edge-based shape detection. *IEEE Transactions on Image Processing*, 11(11):1209–1227.

Noh, H., Hong, S., and Han, B. (2015). Learning deconvolution network for semantic segmentation. *Proceedings of the IEEE International Conference on Computer Vision*, 2015 Inter:1520–1528.

Patterson, J. and Gibson, A. (2017). *Deep Learning - A Practitioner's Approach*.

Pinheiro, P. O., Lin, T. Y., Collobert, R., and Dollár, P. (2016). Learning to refine object segments. *Lecture Notes in Computer Science (including subseries Lecture Notes in Artificial Intelligence and Lecture Notes in Bioinformatics)*, 9905 LNCS:75–91.

Planet (2017). SkySat - Constellations.

Shao, Y., Taff, G. N., and Walsh, S. J. (2011). Shadow detection and building-height estimation using IKONOS data. *International Journal of Remote Sensing*, 32(22):6929–6944.

Simonyan, K. and Zisserman, A. (2014). Very Deep Convolutional Networks for Large-Scale Image Recognition. pages 1–14.

Stanford (2017). Sliding Windows - Stanford University.

Szegedy, C., Liu, W., Jia, Y., Sermanet, P., Reed, S., Anguelov, D., Erhan, D., Vanhoucke, V., Rabinovich, A., Hill, C., and Arbor, A. (2014). Going Deeper with Convolutions. pages 1–9.

Worboys, M. F. (2003). *GIS: A computing perspective*.

Wu, S., Zhong, S., and Liu, Y. (2017). Deep residual learning for image steganalysis. *Multimedia Tools and Applications*, pages 1–17.

Yu, Z., Feng, C., Liu, M.-Y., and Ramalingam, S. (2017). CASENet: Deep Category-Aware Semantic Edge Detection.

Zeiler, M. D. and Fergus, R. (2013). Visualizing and understanding convolutional networks. *Lecture Notes in Computer Science (including subseries Lecture Notes in Artificial Intelligence and Lecture Notes in Bioinformatics)*, 8689 LNCS(PART 1):818–833.

Zeiler, M. D., Taylor, G. W., and Fergus, R. (2011). Adaptive deconvolutional networks for mid and high level feature learning. *Proceedings of the IEEE International Conference on Computer Vision*, pages 2018–2025.